Virology 456-457 (2014) 145–156

Contents lists available at ScienceDirect

Virology

journal homepage: www.elsevier.com/locate/yviro

Vaccinia virus F5 is required for normal plaque morphology in multiple cell lines but not replication in culture or virulence in mice

Bianca M. Dobson [a], Dean J. Procter [b], Natasha A. Hollett [a,1], Inge E.A. Flesch [a], Timothy P. Newsome [b], David C. Tscharke [a,*]

[a] Division of Biomedical Science and Biochemistry, Research School of Biology, The Australian National University, Canberra, ACT, Australia
[b] School of Molecular Bioscience, University of Sydney, Sydney, NSW, Australia

ARTICLE INFO

Article history:
Received 6 December 2013
Returned to author for revisions
29 December 2013
Accepted 19 March 2014
Available online 5 April 2014

Keywords:
Vaccinia virus
Plaque morphology
Cytopathic effect
Cell migration
Modified vaccinia virus Ankara

ABSTRACT

Vaccinia virus (VACV) gene *F5L* was recently identified as a determinant of plaque morphology that is truncated in Modified Vaccinia virus Ankara (MVA). Here we show that *F5L* also affects plaque morphology of the virulent VACV strain Western Reserve (WR) in some, but not all cell lines, and not via previously described mechanisms. Further, despite a reduction in plaque size for VACV WR lacking *F5L* there was no evidence of reduced virus replication or spread *in vitro* or *in vivo*. *In vivo* we examined two mouse models, each with more than one dose and measured signs of disease and virus burden. These data provide an initial characterization of VACV *F5L* in a virulent strain of VACV. Further they show the necessity of testing plaque phenotypes in more than one cell type and provide an example of a VACV gene required for normal plaque morphology but not replication and spread.

Introduction

Infection with vaccinia virus (VACV) disrupts numerous cellular pathways resulting in significant changes in cell morphology. Infection of confluent monolayers of many adherent cell lines with VACV results in the formation of large circular plaques due to a combination of cytopathic effects and migration of infected cells. Three groups of poxvirus genes affect plaque formation. Firstly the many poxvirus genes that are essential for virus replication are therefore required for plaque formation. Secondly, plaque formation is also reliant on spread of infectious extracellular virions (EV) mediated by actin tails. Therefore, loss of proteins involved either in morphogenesis or intracellular transport of wrapped virions (WV), or actin tail formation itself dramatically reduce plaque size despite production of high levels of mature virions (MV). A third group of genes is required for normal plaque morphology and size but less strongly affect virus output *in vitro*. Analysis of members of this third group of genes has led to mechanistic insight into cytoskeletal rearrangements required for cell migration (*F11L*) and attachment to the extracellular matrix (*C2L* and *A55R*)(Pires de Miranda et al., 2003; Beard, et al., 2006; Valderrama et al., 2006; Arakawa et al., 2007a, 2007b; Morales et al., 2008; Cordeiro et al., 2009; Handa et al., 2013).

VACV mutants with reduced plaque size or altered plaque morphology typically show altered virulence. Examples include VACV strain Western Reserve (WR) C16 and B14 (VACWR010/209 and VACWR196 respectively) both of which encode functions required for normal plaque size and for virulence (Chen et al., 2006, 2008; Fahy et al., 2008). Likewise, VACVWR with deletions of BTB/kelch proteins, C2 or A55, forms wild type sized plaques with indistinct borders and causes altered lesions following intradermal infection of mice (Pires de Miranda et al., 2003; Beard et al., 2006). Beyond VACV, plaque size is positively correlated with case fatality rates for variola virus isolates within the same clade (Olson et al., 2009). Data such as these have led to a conventional view that changes to plaque morphology will be mirrored by *in vivo* changes to virus replication, spread and/or virulence.

We have recently identified *F5L* as another VACV gene that influences plaque morphology and spread during a study based on strain Modified Vaccinia virus Ankara (MVA) (Dobson and Tscharke, 2013). MVA fails to replicate on most mammalian cell lines (Carroll and Moss, 1997; Drexler et al., 1998), however using a marker rescue approach, Wyatt et al. (1998) generated a set of recombinant MVAs (rescued MVAs) with improved replication on a range of mammalian cells. We identified *F5L*, which is truncated in MVA but repaired in some of the rescued viruses, as a gene

* Correspondence to: Research School of Biology, Bldg #134 Linnaeus Way, The Australian National University, Canberra ACT 0200, Australia. Tel.: +61 2 6125 3020; fax: +61 2 6125 0313.
E-mail address: David.Tscharke@anu.edu.au (D.C. Tscharke).
[1] Present address: Department of Medical Microbiology, University of Manitoba, Winnipeg, MB, Canada.

http://dx.doi.org/10.1016/j.virol.2014.03.020
0042-6822/

responsible for significant differences in plaque morphology across this set of rescued MVA strains (Dobson and Tscharke, 2013). Further experiments found that while repair of F5 was associated with significant changes in plaque morphology it had no discernible effect on replication *in vitro* (Dobson and Tscharke, 2013). *F5L* remains poorly characterized, but an early description of the VACV *Hind*III F region and the most accurate VACV-genome wide transcriptomic study found that it is expressed early after infection (Roseman and Slabaugh, 1990; Yang et al., 2010). F5 is not a component of mature virions (MV) (Chung et al., 2006; Yoder et al., 2006; Resch et al., 2007; Manes et al., 2008) and a large yeast-two-hybrid study found no interactions between F5 and other VACV proteins (McCraith et al., 2000).

It was possible that the role found for F5 in the context of MVA was influenced by one or more of the many other genetic changes in MVA compared to most virulent VACV strains. Further, studies of virulence based on viruses with the MVA genetic background will be complicated by the loss of many virulence functions, some known and others yet to be defined (Blanchard et al., 1998). Indeed a recent report demonstrated that the rescued MVAs were highly attenuated and the rescued strain with the largest plaque was no more virulent than MVA in an intranasal infection model, even in immunocompromised mice (Melamed et al., 2013). To address these issues, we explored the function of *F5L* in VACVWR. In this virulent VACV strain, F5 is required for normal plaque size and morphology in multiple cell lines, but was not required for replication or spread in any cells *in vitro*, nor for virulence *in vivo*.

Results

Conservation of F5 across the poxviruses and similarity to known proteins

F5L (also annotated as *VACWR044*) encodes a 322 aa protein in VACVWR. F5 contains a predicted signal sequence, with a cleavage site between aa 20 and 21 (Signal P 3.0 (Bendtsen et al., 2004)) and a putative transmembrane domain at the carboxyl-terminus (aa 287-311) (TMHMM (Krogh et al., 2001)). Orthologs are found in all members of the orthopoxvirus genus for which genome sequence is available except ectromelia virus (Viral Orthologous Clusters, (Upton et al., 2003)). The taterapoxvirus homolog is truncated to 193 aa and therefore lacks the putative transmembrane domain (GenBank Accession number NC_008291). No significant homologs are found outside the genus (BLASTp, *E* value < 0.001). Beyond the poxviruses, the amino terminus of F5 contains a region with similarity to immunoglobulin V-set domain containing proteins, but this does not reach the significance threshold (*E* value = 0.00036) (Pfam (Finn et al., 2010)). Variation exists amongst *F5*L homologs from various strains of VACV (Fig. S1). For example, *F5L* from the VACV strain referred to as Ankara, used to rescue MVA for growth on BS-C-1 cells (Wyatt et al., 1998) and for our description of a role for F5 in the context of MVA (Dobson and Tscharke, 2013), encodes a 321 amino acid protein due to a 3 bp deletion. In addition to this difference, 10 nucleotide substitutions are present in Ankara *F5L* compared with VACVWR, resulting in four amino acid changes.

Deletion of F5L affects plaque morphology but not replication of VACVWR

A VACVWR strain with 86% of the *F5L* ORF deleted (VACVWRΔF5L) and a revertant (VACVWRF5Lrev) were made, demonstrating that F5 is non-essential for VACVWR growth in culture. However, plaques formed by VACVWRΔF5L were approximately 30% smaller than the parent or VACVWRF5Lrev on BS-C-1 cells. Cell clearance from the center of plaques was reduced and the distinctive halo of contracted cells that usually surround VACV plaques (Cordeiro et al., 2009) was absent (Fig. 1a and d). Further, live microscopy showed that the expansion rate of plaques was slower in the absence of F5 (Fig. 1c). VACVWRΔF5L also formed smaller plaques on RK13, IEC-6, and 293A cells (Fig. 1b,e,f and 6b). By contrast, we observed no difference in plaques formed on primary human foreskin fibroblasts, BHK-21 or the murine cell line NIH/3T3 (Fig. 1b, and data not shown).

To determine whether loss of F5 affected virus replication, a high multiplicity (m.o.i. = 5) growth experiment was done (Fig. 2a). This found no decrease in replication associated with the loss of F5. We then used multiple-step experiments (m.o.i. = 0.01) to measure replication and spread. These found that deletion of *F5L* had no effect on either cell associated, or supernatant virus yield in BS-C-1 (Fig. 2b) or primary human foreskin fibroblasts (HFF) (data not shown). To probe replication and spread more stringently, inocula were reduced to approximately 50 p.f.u. in a 9.5 cm^2 culture of BS-C-1, so that spread would not be inhibited by a lack of infectable cells. Even in this experiment with six replicates, no statistically significant difference in virus output per plaque was across the parent, VACVWRΔF5L and VACVWRF5Lrev or between any pair of viruses at 72 h post infection (h.p.i.)(Fig. 2c). This last experiment was repeated and again no significant differences were found. Taken together, these experiments suggest that F5 has no discernible role in VACVWR replication or spread in *in vitro* culture, even on a cell line where it is required for normal plaque morphology.

Localization of the F5 protein in infected cells

In order to test the predicted cell membrane localization of F5 we produced VACVWR/F5LGFP in which the native F5 was replaced with an F5-eGFP fusion. This virus had a plaque phenotype similar to VACVWR on BS-C-1 cells (Fig. S2), demonstrating that F5 function is intact in this virus. There was diffuse fluorescence in cells infected with VACVWR/F5LGFP at several times after infection up to 8 h.p.i., but across multiple images we were unable to determine the localization with any certainty. The only common pattern that was evident across all images emerged from 6 to 8 h. p.i. and was an enrichment of eGFP at the periphery of the cell where thin cytoplasmic extensions are evident. This localization was restricted to regions in contact with neighboring cells, suggesting cell–cell contact might stabilize or recruit F5 (Fig. 3). This pattern of staining was not seen in cells infected by VACVWR expressing eGFP not fused to *F5L*, but was confirmed for F5-eGFP by total internal reflection fluorescence (TIRF) microscopy (not shown). To further define the location of F5-eGFP fluorescence, cells were stained for actin (phalloidin and cortactin), the cell-to-cell junction marker β-catenin, or phosphotyrosine as a marker of focal adhesions. In each case projections marked with eGFP were noted, but these failed to co-localize with any of the host cell markers (Fig. 3). Finally, F5-eGFP did not colocalize with B5, a marker for enveloped virus (EV) or the virus factory, as shown by the DNA stain DAPI, where intracellular mature virus is assembled (Fig. 3 row 3 and other rows respectively).

F5L is not required for actin tail formation, Ca^{2+} independent cell adhesion or cell migration

Deletion of viral genes has identified three mechanisms associated with alterations in VACV plaque size and appearance which are not always matched by a measureable reduction in virus yield: (1) ability to make actin tails, (2) loss of adhesion of infected cells in the absence of Ca^{2+} and (3) altered cell migration of infected

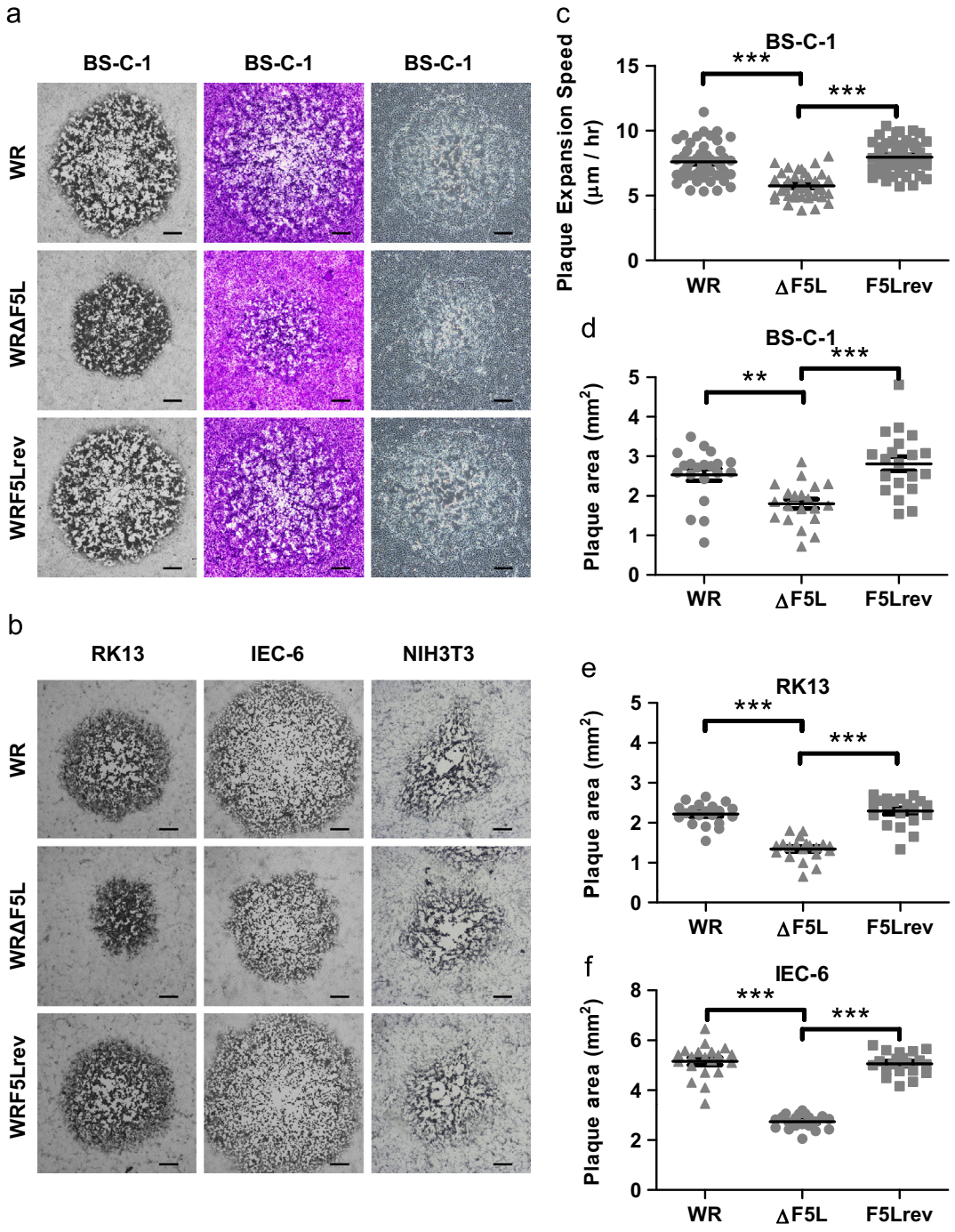

Fig. 1. Deletion of F5L affects plaque phenotype on several cell lines. Plaque formation on BS-C-1, RK13, IEC-6 or NIH/3T3 cells by VACVWR, VACVWRΔF5L and VACVWRF5Lrev. (a and b) Representative plaques formed under semisolid media were immunostained, crystal violet stained or photographed unstained. Scale bar 300 μm. (Original magnification: 40 ×). (c) Average plaque expansion speed on BS-C-1 is indicated by the solid line. The expansion of the leading edge of plaques was monitored from 16 to 56 h.p.i. using live-cell microscopy. One-way ANOVA ($n=53$, $P<0.0001$) and Tukey pairwise test (***$p<0.001$). (d–f) Average area of immunostained plaques formed under semisolid media on BS-C-1, RK13 or IEC-6 is indicated by the solid line. One-way ANOVA ($n=20$) and Tukey pairwise test (** $p<0.01$, ***$p<0.001$). (e).

cells. We considered whether deletion of F5 might act by these mechanisms, addressing each in turn below.

1. VACV morphogenesis is complicated and several forms of infectious virus are made. The form of virus implicated in virus spread *in vivo* is wrapped with an additional membrane (EV) and is able to be released from infected cells, or propelled into a neighboring cell by an actin tail (Roberts and Smith, 2008; Welch and Way, 2013). Loss of certain proteins incorporated into the outer membrane of EV dramatically reduces plaque size as a result of decreased EV production, reduced infectivity of the virus released, or decreased production of actin tails (Blasco and Moss, 1991; Duncan and Smith, 1992; Engelstad and Smith, 1993; Wolffe et al., 1993, 1997; McIntosh and Smith, 1996; Roper et al., 1998; Ward and Moss, 2001). Likewise, viruses lacking other genes required for efficient assembly and transport of WV or for actin tail formation, have very small plaques (Rodriguez and Smith, 1990; Parkinson and Smith, 1994; Wolffe et al., 1998; Zhang et al., 2000; van Eijl et al., 2002; Domi et al., 2008; Dodding et al., 2009; Morgan et al., 2010). We noted that the effect of *F5L* on plaque size

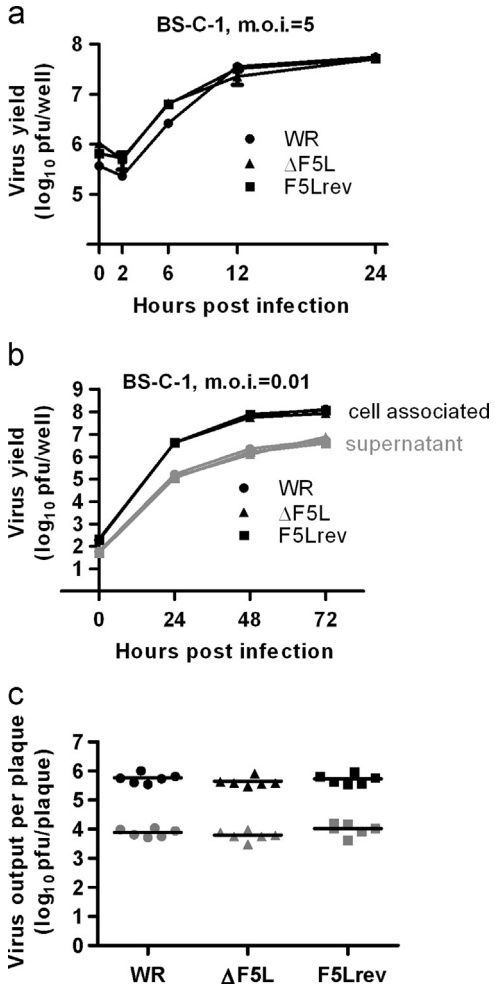

Fig. 2. Deletion of F5L does not affect replication *in vitro*. (a) Single step growth analysis (m.o.i.=5) in BS-C-1, cell associated virus is shown. (b) Multiple step growth analysis (m.o.i.=0.01) in BS-C-1, cell associated virus shown in black, virus in the supernatant is in gray. Data points are representative of three independent wells. Mean ± SEM. (c) Average virus yield per plaque 72 hpi after infection of BS-C-1 with approximately 50 pfu/well is indicated by the solid line. Cell associated virus shown in black, virus in the supernatant is in gray.

was not as strong as published reports for these genes. Furthermore, F5 appeared not to be required for EV production and release because similar amounts of virus were found in the supernatant of cells infected with VACVWRΔF5L, its parent and the revertant (Fig. 2b). When 'comet' plaque assays were done with liquid overlay so that secondary plaques can be formed by released EV, the morphology of the primary and small secondary plaques but not the extent of secondary plaque formation was dependent on F5 (data not shown). Finally, actin tails were observed directly for our viruses. As shown in Fig. 4a, no significant difference in actin tail length was found between VACVWRΔF5L and VACVWRF5Lrev (Fig. 4a).

2. When Ca^{2+} is depleted from the growth medium, uninfected BS-C-1 cells lose the ability to adhere to the extracellular matrix and round up, but this process is inhibited by VACV infection (Sanderson and Smith, 1998). The A55 and C2 proteins of VACVWR are required for VACV-induced Ca^{2+}-independent cell adhesion. Like *F5L*, deletion of *C2L* or *A55R* alters plaque morphology without substantially affecting *in vitro* replication and plaques formed by VACVWRΔF5L appeared similar to published images of the VACVWR mutants, vΔC2 and vΔA55, so we wondered if F5 was required for Ca^{2+}-independent adhesion (Pires de Miranda et al., 2003; Beard et al., 2006). BS-C-1 cells were infected with VACVWR, VACVWRΔF5L, or VACVWRF5Lrev for 18 h before Ca^{2+} was sequestered by adding EDTA to the medium and then adhesion of cells was monitored over 20 min (Fig. 4b). Uninfected cells rapidly lost adhesion and rounded up. By contrast, the majority of virus-infected cells remained strongly adherent and the absence of F5 had no effect on this Ca^{2+}-independent adhesion.
3. VACV infection induces migration of cells and protein F11 is involved in the cytoskeletal rearrangements required for this motility (Valderrama et al., 2006; Morales et al., 2008; Cordeiro et al., 2009; Handa et al., 2013). As a result, deletion of *F11L* from VACVWR reduces plaque size (Morales et al., 2008; Cordeiro et al., 2009; Handa et al., 2013) and cells infected with MVA, in which *F11L* is fragmented, do not migrate into a wound made in a monolayer of serum starved BS-C-1 cells (Valderrama et al., 2006; Zwilling et al., 2010). Initial live microscopy suggested that F5 was not required for cell motility (not shown) but to test this more quantitatively we measured migration of BS-C-1 cells infected with VACVWRΔF5L, VACWRF5Lrev, or VACVWR using a scratch wound assay (Fig. 5a and b). Compared to mock-infection, all viruses induced significant migration of cells into the wound, irrespective of deletion of *F5L*. To ensure that this assay was sensitive to impairment of migration, we extended the assay to include several viruses based on MVA made in the process of mapping F5 as a determinant of plaque morphology in this strain. These viruses were v51.2/F11LGb, in which *F11L* was repaired; v51.2/F5LGb and v51.2/F5L, in which *F5L* was repaired; v51.2/F5L-F11L, in which *F5L* and *F11L* were repaired ((viruses with 'Gb' in their name retain a GFP/bsd selectable marker downstream of the repaired gene) (Dobson and Tscharke, 2013). In agreement with the literature, only cells infected with viruses that had an intact *F11L* gene migrated into the wound. Presence or absence of F5 had no impact on migration either alone or in combination with F11 across this set of viruses (Fig. 5c).

Virus infection is needed for F5 stability, but the predicted cytoplasmic tail is not required for function in vitro

In order to study the effect of F5 expression on uninfected cells, we produced two F5-eGFP fusions expressed from the CMV IE promoter. The fusions contained either a full length (322 aa) or truncated (218 aa) *F5L* from VACVWR and were tagged on their c-termini with eGFP (pEGFP-N1::F5L and pEGFP-N1::F5L218, respectively). F5L218 contains at Ser218Pro mutation such that the protein produced is identical to the predicted MVA F5 homolog (MVA034), and lacks 104 aa of the c-terminus, including the putative transmembrane domain. No differences in cell morphology were observed between 293A cells transfected with pEGFP-N1::F5L, pEGFP-N1::F5L218 or the empty control vector (not shown). The brightness of fluorescence in cells transfected with these constructs was in the order, empty pEGFP-N1 > pEGFP-N1::F5L218» pEGFP-N1::F5L. To test if F5-eGFP instability in uninfected cells was contributing to the weak fluorescence, cells were mock-infected or infected with VACVWRΔF5L, 3 h after transfection (Fig. 6a). Infection greatly increased fluorescence in cells expressing full length F5-eGFP, despite this construct being under control of the CMV IE promoter. By contrast and as expected for genes transcribed from the nucleus, eGFP fluorescence from theF5L218-GFP and the empty vector control construct was reduced by VACV infection. Thus the order of brightness after VACV infection was pEGFP-N1::F5L » empty pEGFP-N1 and pEGFP-N1::F5L218. In further experiments, F5L-eGFP brightness, but not that of the other two constructs was improved by VACVWR infection in the presence of AraC (data not shown). Together these experiments

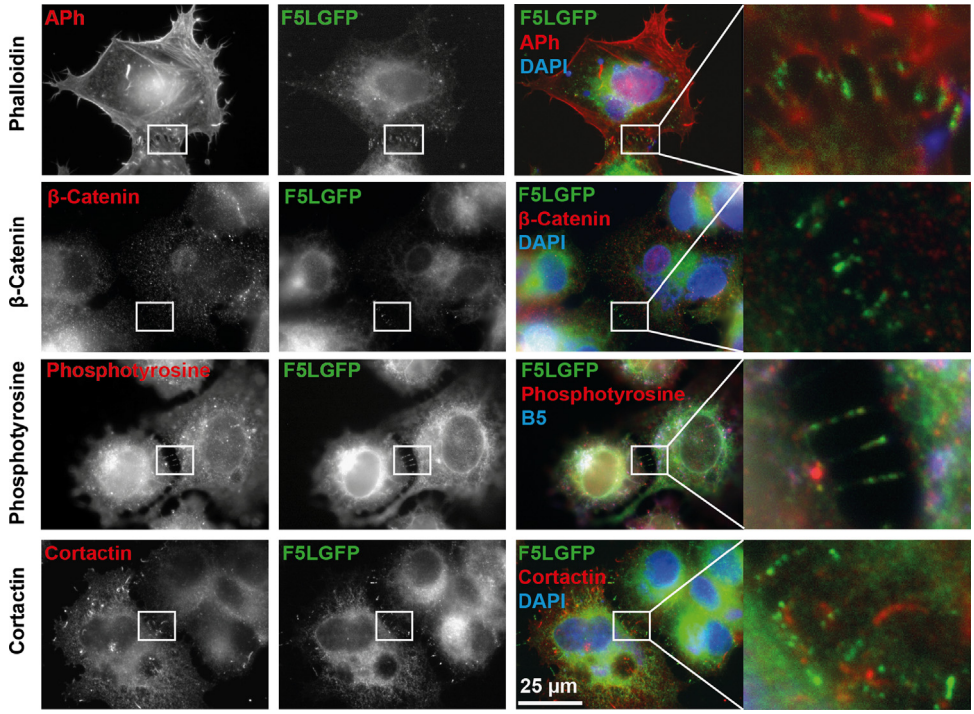

Fig. 3. Localization of F5. HeLa cells were infected with VACVWR/F5LGFP (m.o.i. = 5) fixed at 8 h.p.i., stained with Alexa Fluor 568-phalloidin (Aph, actin), anti-β-catenin (cell-to-cell junctions), anti-phosphotyrosine (focal adhesions) or anti-cortactin (actin-cytoskeleton rearrangements) along with DAPI or anti-VACV-B5 (B5) (row 3) and imaged (100 × objective) to analyze the localization of F5L-GFP.

suggest that full length F5 requires another function expressed early in VACV infection for stability in cells, but this depends on sequences in *F5L* from WR that are not present in the truncated version expressed by MVA.

Next, a complementation assay was used in which F5L fused to GFP was expressed from a plasmid under its natural promoter in cells infected by VACVWR or VACVWRΔF5L to determine if any domains were dispensable for function. Similar complementation assays have been used by others, including for genes with VACV early promoters, even though the early transcription factors are thought to be mostly sequestered in the virus cores (Cochran et al., 1985; Valderrama et al., 2006). The plasmid also encoded mCherry under the VACV strong synthetic promoter (pSS), which was brighter than F5-eGFP to more easily identify cells that received virus and the plasmid at low magnification. A plasmid containing F5-eGFP, but not the empty vector was able to rescue the plaque defect of VACVWRΔF5L on 293A cells demonstrating expression of functional F5 (Fig. 6b). Next, we tested the ability of a set of plasmids expressing F5-eGFP with regions of F5 deleted to rescue the plaque defect of VACVWRΔF5L. The predicted features of F5 covered by these deletions were the signal sequence, the extracellular domains (broken into four segments) and the short cytoplasmic tail (Fig. 6c). Of these constructs, only the cytoplasmic tail deletion was still able to rescue the plaque size of VACVWRΔF5L, but eGFP fluorescence was always seen (Fig. S3). These experiments suggest that the putative cytoplasmic tail is not required for the function of F5 in plaque morphology.

F5L does not affect VACV pathogenesis, replication or spread in mice

We examined the role of F5 in VACV virulence using two murine models of infection. First, BALB/c mice were infected intradermally with VACVWR, VACVWRΔF5L or VACVWRF5Lrev and lesion size monitored over 21 days (Fig. 7a). All viruses produced lesions at the infection site, but there was no difference in size between VACVWRΔF5L and controls. Virus replication over the first 5 days was also tested in this model, with doses of 1×10^4 p.f.u. and 1×10^2 p.f.u.. A titer of around 1×10^7 p.f.u. was achieved irrespective of inoculum or virus, showing that F5 does not increase VACV replication *in vivo* in mice (Fig. 7b).

Second, the intranasal model of infection was used. Three experiments were done with a dose of 1×10^4 p.f.u. and there were no statistically significant differences in weight loss or number of mice that were euthanized due to loss of $>30\%$ of starting weight between VACVWRΔF5L and the control viruses (Fig. 8a). A lower dose of 1×10^3 p.f.u. was then used to tease out any small difference between viruses, but again no consistent phenotype was found for VACVWRΔF5L (Fig. 8a). Virus titers were measured at 3, 7 and 10 days after intranasal infection with 1×10^4 p.f.u. of VACVWR, or VACVWRF5Lrev, examining lungs, brain, spleen (Fig. 8b), ovaries and liver (not shown). No significant difference in titer was found between the groups of mice for any organ at any time. Finally we tested several parameters of immunity in mice infected intranasally with VACVWRΔF5L and controls. There were no differences in: (a) the total VACV-specific IgG response as measured by ELISA (Tscharke et al., 2002); (b) the memory $CD8^+$ T cell response in the spleen as measured by production of IFN-γ after stimulation with VACV peptide epitopes (Flesch et al., 2012a, 2012b); (c) infiltrates present in brochoalveolar lavage taken at various times after infection (Reading and Smith, 2003) (data not shown).

Discussion

We demonstrate here that VACV gene *F5L* is a determinant of plaque morphology in VACVWR when grown on a subset of cell lines tested, but does not contribute to virus replication *in vitro* in these same cells or to pathogenesis in mice. Taken at face value, smaller plaques in the absence of F5 suggest that this protein is required for normal spread of virus. However, no detectable change to replication *in vitro* was found despite using very low input titers to maximize the

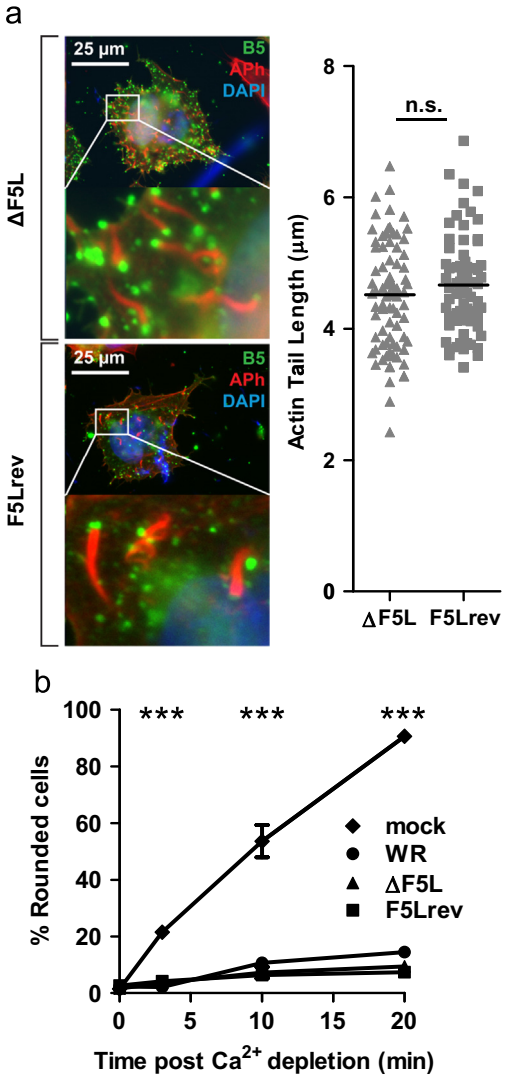

Fig. 4. F5 does not affect formation of actin tails, or calcium independent cell adhesion. (a) Length of individual actin tails ($n=74$) were measured from micrographs of infected HeLa cells (100 × objective). 8 h.p.i. nonpermeabilized cells were stained with anti-B5 (green) and Alexa Fluor 568-phalloidin (red) to identify extracellular virus and virus-induced actin tails. Solid line indicates mean. n.s., no significant difference was found between the means. (b) Ca^{2+} independent cell adhesion. Monolayers of BS-C-1 cells infected (m.o.i.=3) or mock infected, were treated with 10 mM EDTA at 18 h.p.i. Percentage of rounded up cells was calculated from three micrographs per time point. At least 155 cells were counted in each micrograph (***Mock infected cells significantly different to infected cells, $p<0.001$, Two-way ANOVA, Bonferroni post test).

influence of virus spread. In addition, there was no defect in the ability of VACVWRΔF5L to replicate at primary sites of infection in mice, as seen in skin and lungs after intradermal and intranasal infection respectively, nor was there a defect in virus dissemination. In the case of the intradermal infection the above held true where the inoculated dose was as low as 100 p.f.u. and virus growth exceeded five orders of magnitude in 5 days, a very robust test of replication *in vivo*. It remains possible that deletion of *F5L* is associated with a very subtle reduction in virus production or spread that was beyond our sensitivity to dissect, but it is unclear that such a small difference would be important for the outcome of infection. Another important point highlighted by this study is that the effects of virus genes on plaques can be cell type-specific. We observed no difference in plaque size or morphology between VACVWRΔF5L and the wild type VACVWR when grown on BHK-21 (hamster), NIH/3T3 (mouse), or HFF (human), in contrast to the clear and reproducible differences seen for BS-C-1 (African green monkey), RK13 (rabbit), IEC-6 (rat) and 293A (human) (Figs. 1 and 6b). A further set of cell lines including HeLa (human), Vero (African green monkey), L-cells (mouse) and L-Db (derivative of L-cells) made small and relatively variable plaques, or only foci, with all viruses making assessment of morphological differences associated with F5 inconclusive. There is no obvious species specificity across this wide range of cells, but some correlation with cell shape was noticed: F5 affected the round, regular plaques formed on cells that have cobble-stone or cuboid shapes when confluent and uninfected. By contrast, F5 had no affect on cells with more elongated (primary fibroblastoid-like) forms when confluent and on which VACV makes somewhat irregular plaques. This observation may have some relevance for the function of F5.

A range of VACV genes has been characterized as being required for normal plaque morphology but when deleted have a minor (less than 10-fold) or undetectable effect on virus yield in multiple step growth curves. These include *A55R*, *C2L* (indistinct borders on BS-C-1) (Pires de Miranda et al., 2003; Beard, Froggatt, and Smith, 2006); *C11R* (10–30% smaller plaques on BS-C-1) (Buller et al., 1988), *VACVWR010/209* (approximately 20–30% smaller plaques on BS-C-1 and RK13) (Fahy et al., 2008), *O1L* (plaques approximately 50% smaller on 293A) (Schweneker et al., 2012) and *VACWR196* (smaller plaques on BSC-1 (20%) and CV-1(40%)) (Chen et al., 2006). However, in each case viruses lacking these genes had altered pathogenesis in at least one model of infection in mice. In contrast for F5, over a total of six experiments across two models, no consistent role in virulence was observed, nor could an influence of this protein be found on three parameters of the immune response. The only other VACV protein associated with a plaque phenotype and not virulence is another membrane associated protein, A38, but pathogenesis was only assessed in a single model (Parkinson et al., 1995). There is a range of other VACV genes for which deletion does not change pathogenesis in mice, for example *A45R*, *B9R* and *B12R*, but in these cases there is a similar lack of phenotype for the deletion virus *in vitro* (Banham and Smith, 1993; Almazan et al., 2001; Price et al., 2002; Tscharke et al., 2002). An example of a VACV protein with a known function that fails to alter pathogenesis in well controlled studies in mice is B8. B8 binds IFNγ from many species, but not mice, explaining its lack of function in mouse models (Alcamí and Smith, 1995; Symons et al., 2002). However, the *B8R* ortholog in the mouse-specific pathogen ectromelia virus does bind mouse IFNγ and deletion from this virus reduces virulence (Sakala et al., 2007). We speculate that F5 may lack a binding partner in this species, in support of this we saw no plaque defect in the absence of F5 on mouse NIH/3T3 cells, although we did observe a difference on another rodent cell line, IEC-6. It is interesting to note that ectromelia virus, a mouse-specific orthopoxvirus lacks an *F5L* homolog. However, at the same time a role for virulence in mice has been shown for VACV genes *K7R* and *A40R* that are fragmented and therefore also non-functional in ectromelia virus (Tscharke et al., 2002; Benfield et al., 2013). It remains unlikely that VACV would maintain a gene that has no role in an *in vivo* setting, therefore it may be of value to investigate F5 function in another host species. Assuming such a function is found, it would be of interest to determine if it can be related in any way to the role for F5 revealed in plaque morphology here.

While we have not defined how F5 contributes to plaque formation, its role is non-redundant and its mode of action is distinct from previously defined mechanisms. Firstly, there was no evidence that F5 plays any role in virion morphogenesis, EV release or actin tail formation. Secondly, unlike F11, F5 did not affect cell motility as captured by a scratch wound assays. Finally, unlike *C2L* or *A55R*, deletion of *F5L* from VACVWR does not reduce Ca^{2+}-independent binding of cells to extracellular matrix. From the predicted structure, apparent localization to cell–cell contacts

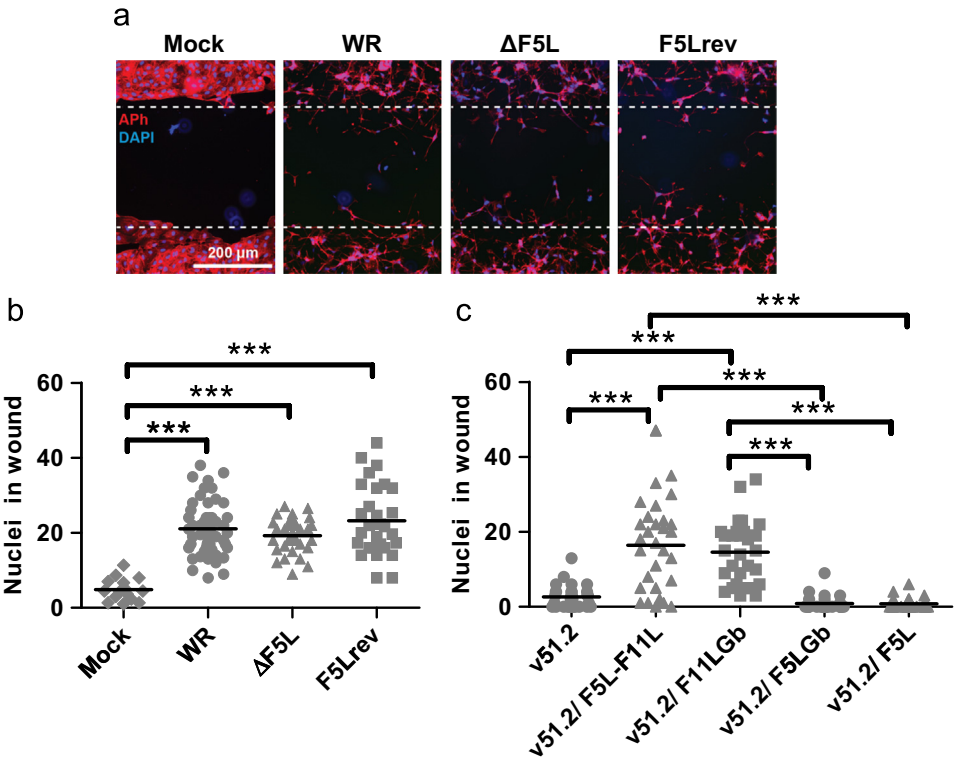

Fig. 5. F5L is not required for VACV-induced cell migration. Wound healing assay: Wounds were created 1 h.p.i. in serum starved BS-C-1 monolayers. 24 h.p.i. cells were stained with DAPI (blue) and Alexa Fluor 568-phalloidin (red). (a) Dotted lines indicate average wound size as determined for mock infected cells, the viruses used for infection are shown above each micrograph. (b–c) Number of cells with DAPI-stained nuclei within the average wound size for the viruses noted on the *x*-axis. Means are indicated by solid lines. (b) One-way ANOVA ($P < 0.0001$) and Tukey pairwise test (*** $p < 0.05$). (c) One-way ANOVA ($P < 0.0001$) and Tukey pairwise test (***$p < 0.05$).

and lack of requirement for the putative intracellular portion we speculate that F5 functions via interactions with proteins on neighboring cells or extracellular matrix elements. However, this remains to be determined.

In summary, we identify F5 as a determinant of plaque phenotype in a virulent strain of VACV and the data presented provide a foundation for further work on this previously uncharacterized protein. Finally, our investigations of *F5L* are a reminder that small plaque phenotypes should be checked in multiple cell lines and cannot always be assumed to be a correlate of virus replication and spread.

Methods

Cells and virus

All cells were maintained in Dulbecco's modified Eagle medium (DMEM; Gibco/Invitrogen) with L-glutamine and 10% FBS (D10), except for BHK-21 (Minimum Essential Medium (Gibco/Invitrogen) with L-glutamine and 10% FBS). Lipofectamine 2000 (Invitrogen) was used for all transfections. VACV stocks were grown in BHK-21 in DMEM with L-glutamine and 2% FBS (D2) and purified by centrifugation through a 36% sucrose cushion. Virus titers were determined by plaque assay on BS-C-1.

Plasmid construction

PCR was used to generate inserts for InFusion (Clontech) or conventional cloning. In descriptions below, PCR primers for (a) InFusion contain 15 bp matching flanking vector sequence (underlined) or a neighboring insert (bold); (b) conventional ligations include restriction enzyme sites (italics).

Generation of recombinant VACV

General strategy: All recombinant VACV were produced by infection of 293A cells with the appropriate parent virus (m.o.i.=0.05) followed by transfection 1 h later with 1 μg of plasmid DNA. After 2 h at 37 °C transfection media was replaced with 2 ml D2. Cells were harvested 2 days later. Plaque purification was carried out on BS-C-1 in phenol-red free D2-CMC. PCR screening and sequencing was used to confirm the correct modification had occurred and identify plaque picks free of parental virus. Two independent recombinant viruses were isolated from parallel infection/transfection experiments.

VACVWRΔF5L and VACVWRF5Lrev: VACVWRΔF5L was engineered using transient dominant selection for the GFP-*bsd* marker gene from plasmid pSSGb (Wong et al., 2011). Sequences flanking *F5L* were amplified from VACVWR DNA with: Left flank: F5LLfwd: CAGTGTGCTGGAATTCTCACTATTCCGTCACTGGCTG and **TTAAACCGCATCAAG**CAGCACCCATGAATGTCGAT; Right: **CTTGATGCGGTTTAA**TAAATG TT and F5LRrev: GATATCTGCA*GAATTC*TGCTGTGGTAGATTCTGTGACG. The last 134bp of *F5L* were preserved to maintain the promoter of *F4L*. VACVWRF5Lrev was produced by recombination between a linearized pSSGb vector containing the full *F5L* reading frame plus homology arms (PCR product of F5LLfwd and F5LRrev) and the VACVWRΔF5L genome.

VACVWR/F5LGFP: To produce an eGFP-tagged version of the F5 protein, a plasmid construct (pSSmCB::F5LGFPnoM) was created with *F5L* fused to the 5′ end of EGFP (without initiation codon), plus the left and right flanking sequences used in the production of VACVWRΔF5L. The left flank (homL) was amplified from VACVWR DNA using TCTAGAGTCGCGGCCTCACTATTCCGTCAC

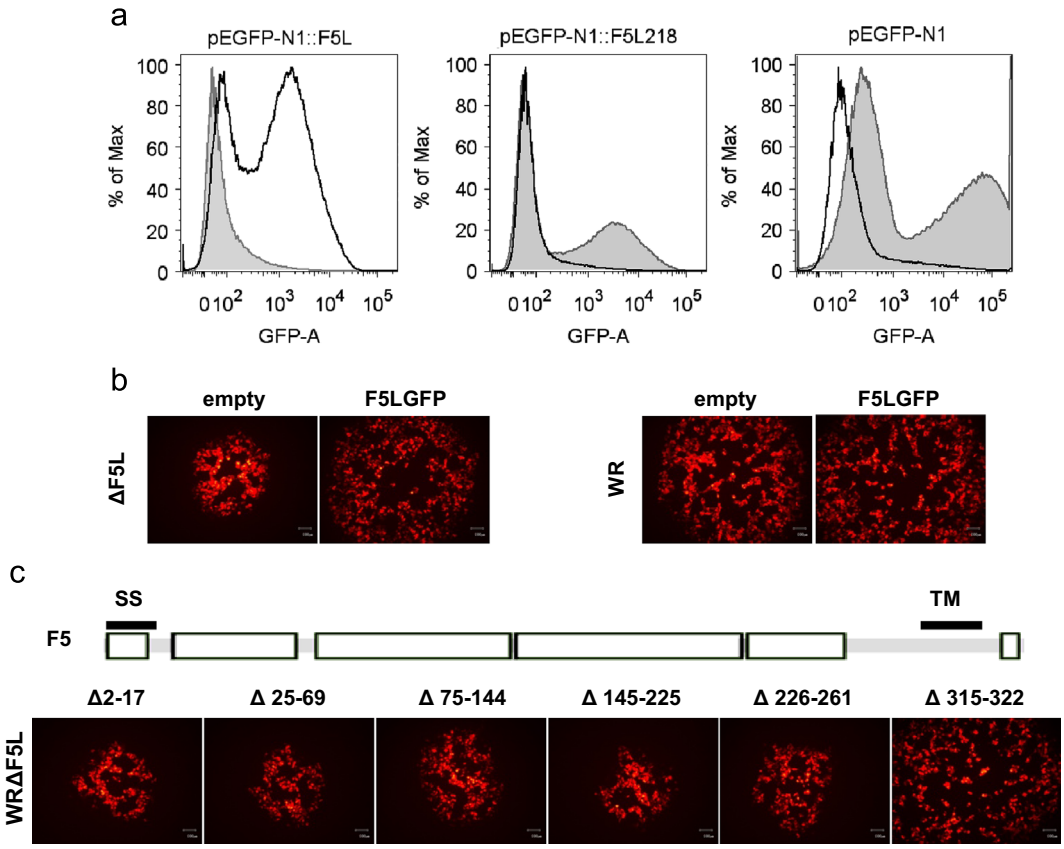

Fig. 6. Virus infection is required for stability and the putative cytoplasmic carboxyl-terminal of F5 is not required for function. (a) Flow cytometry analysis of 293 A cells transfected with vectors expressing GFP fused to VACVWR-length F5L (pEGFP-N1::F5L), GFP fused to MVA-length F5L (pEGFP-N1::F5L218) or GFP only (pEGFP-N1), then infected with VACVWRΔF5L (black line) or mock infected (gray shaded). (b) Typical plaque morphology on 293A cell in the presence or absence of F5 provided by VACV or complemented by a transfected plasmid expressing F5 under its natural promoter. Cells were infected with either VACVWR (right pair) or VACVWRΔF5L (left pair), then transfected with vectors containing full length F5L fused to GFP (F5LGFP) or an empty control vector. mCherry under the VACV pSS, marks virus-infected cells. (c) As for b, except various deletions of F5 were expressed. The deletions are shown on the line diagram (SS, signal sequence; TM, transmembrane domain), with aa deleted noted above each micrograph.

TGGCTG and ACAAGTAAAGCGGCCTTGTAGTGATTGCGGCGAT and cloned into pEGFP-N1 linearized with *NotI;* producing pEGFP-N1::homL. The eGFP gene from the second codon plus homL was then amplified using pGFP: GTGAGCAAGGGCGAGGAG and F5LLfwd. The *F5L* ORF along with the right homology arm was amplified from VACVWR DNA using CTCGCCCTTGCTCACGTTATC-TATATGCCTGTACTTGGAT and F5LRrev. The eGFP-homL and F5L PCR products were cloned into the unique *EcoRI* site in the MCS of pSSmCB (pSSGb from Wong et al., 2011 with eGFP replaced by mCherry). After recombination with VACVWRΔF5L, GFP^+ plaques with wild type plaque morphology were selected.

Evaluation of VACV plaques

Plaque size: confluent cell monolayers in six-well plates were infected with 50 p.f.u. virus. After 2 h at 37 °C, the inoculum was replaced with semisolid D2+0.4% (w/v) carboxy-methyl cellulose (D2-CMC). Cells were fixed and immunostained with anti-MVA antibody followed by an anti-rabbit secondary antibody conjugated to horseradish peroxidase (Staib et al., 2004). Plaque-expansion speed: Confluent BS-C-1 monolayers were infected with 50 p.f.u in glass-bottom six-well plates (MatTek). After 1 h, cells were washed with PBS and Leibovitz's L-15 (Invitrogen) with L-glutamine and 10% FBS was added. Plaques were identified in the monolayers from 14 h.p.i. and the leading-edge of each plaque was imaged every hour from 16 to 56 h.p.i. using an Olympus CellR Live-Cell Microscope (5× objective). Plaque areas and expansion speeds ($\mu m\ h^{-1}$) were calculated for each virus strain using Image J (v1.46j) (Rasband, 1997-2012).

Replication in vitro

Confluent monolayers in six-well plates were infected with either 1×10^4 p.f.u. (multiple step growth curve; m.o.i.=0.01) or 5×10^6 p.f.u (single step growth curve; m.o.i.=5) virus in 1 ml D2. After 1 h at 37 °C, unabsorbed virus was removed, cell monolayer washed once, and 2 ml fresh media added. 0 h samples were harvested immediately after addition of fresh media. Further wells were harvested at the indicated time points. Cells were harvested into existing media, centrifuged at 931 *g* for 10 min to separate cell-associated and supernatant virus, which were titrated separately. To calculate mean virus output per plaque, 9.5 cm^2 wells of confluent BS-C-1 were infected with 500 μl of virus diluted to 1×10^2 p.f.u./ml in D2. After 90 min, the inoculum was replaced with 2 ml D2 without CMC (6 wells per virus), or D2-CMC (3 wells per virus). 72 h.p.i. wells without CMC were harvested and virus titrated. Wells with D2-CMC were stained with crystal violet and plaques counted.

Antibodies and fluorescent chemicals

Primary antibodies used for immunofluorescence assays were anti-B5 (Schmelz et al., 1994), anti-phosphotyrosine (4G10; Chemicon), anti-cortactin (4F11, Upstate Biotechnology), anti-ß-catenin (610154, BD Transduction Laboratories). The secondary

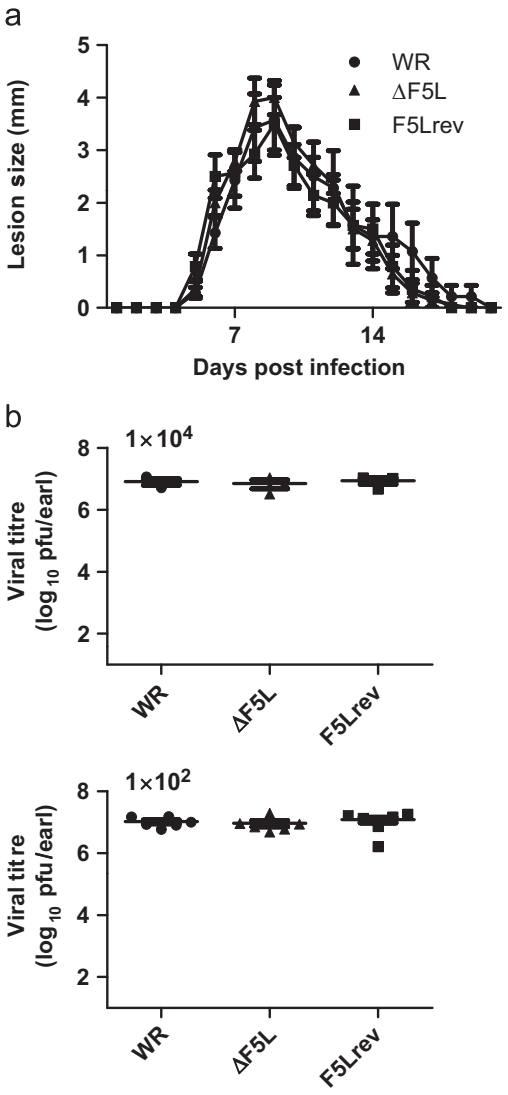

Fig. 7. Deletion of F5L does not affect the virulence of VACVWR after intradermal infection. Eight week old BALB/c mice were infected with VACVWR, VACVWRΔF5L or VACVWRF5Lrev by intradermal injection into the ear pinnae. (a) Lesion size estimated daily to the nearest 0.5 mm after infection with 1×10^4 p.f.u. ($n=6$). Data points are mean ± SEM. (b) Virus titer in the infected ear 5 days p.i. with 1×10^4p.f.u. ($n=3$) or 1×10^2p.f.u. ($n=6$). Titers for individual mice are shown by the symbols and average (± SEM) by solid lines.

antibodies (Invitrogen) were Alexa Fluor 568-conjugated goat anti-mouse IgG, Alexa Fluor 568-conjugated goat anti-rabbit IgG, and Alexa Fluor 350-conjugated goat anti-rat IgG. Fluorescent chemicals used were DAPI (Sigma-Aldrich) (1 μg ml^{-1}) and Alexa Fluor 568-phalloidin (Invitrogen) (1:300 dilution). All antibodies were diluted in blocking buffer (1% BSA and 2% FBS in cytoskeletal buffer (CB) [10 mM MES buffer, 0.15 M NaCl, 5 mM EGTA, 5 mM MgCl2, 50 mM glucose, pH 6.1]).

Immunofluorescence microscopy

Cells were seeded on glass coverslips, infected with appropriate viruses and fixed at 8 h.p.i. with 3% paraformaldehyde (PFA) in CB for 10 min at room temperature. Before staining, cells were permeabilized with 0.1% Triton X-100 in CB (or not permeabilized as indicated). Cells were incubated in blocking buffer for 20 min, suitable primary antibodies for 40 min, washed three times in PBS, then incubated in secondary antibodies for 20 min. The coverslips were mounted on a glass slide with 1% (w/v) p-phenylenediamine (Sigma-Aldrich) in Mowiol mounting medium (10% (w/v) polyvinyl alcohol 4-88 [Sigma-Aldrich], 25% (w/v) glycerol, 0.1 M Tris, pH 8.5). Fluorescence was performed with an Olympus microscope BX51 with filter sets 31001, 31002, and 31013v2 (Chroma). Actin-tail lengths were measured with Image J (v1.46j).

Wound healing assays

Confluent BS-C-1 cells on glass coverslips were serum starved in DMEM without FBS (D0) for 2 h, then infected (m.o.i.=5). 1 h.p.i., wounds were created with a yellow tip and cells were washed in PBS and rescued in D0. Cells were fixed at 24 h.p.i. with 3% PFA in CB for 10 min, stained with DAPI and Alexa Fluor 568-phalloidin and mounted (as described above). All wounds were imaged with an Olympus microscope BX51 (10× objective), and an average wound size was calculated for mock infected cells. The number of cells containing DAPI stained nuclei within each wound was counted.

Calcium independent cell adhesion

Extracellular calcium was depleted by addition of EDTA (Sanderson and Smith, 1998). Confluent BS-C-1 monolayers were infected with the appropriate virus (m.o.i.=3). 18 h.p.i. cells were washed three times with PBS, then 1 ml of PBS containing 10 mM EDTA was added to each well. Cells were incubated at 37 °C for 3, 10 or 20 min. Photographs of three randomly selected fields were taken on a phase contrast microscope (100× magnification). Rounded up and adherent cells in the top left quadrant of each image were counted (155–450 cells).

Transient rescue of VACVWRΔF5L plaque morphology

pSSmCB::F5LGFP encodes the full length F5L-GFP fusion under the F5L promoter. F5L-GFP fusion and promoter were amplified from pSSmCB::F5LGFPnoM with EGFPstop: CAGTGTGCTGGAATTCTTACTTGTACAGCTCGTCCATG and F5LRrev, and cloned into pSSmCB linearized with *Eco*RI. From pSSmCB::F5LGFP five further plasmids were constructed by amplification of the whole plasmid using phosphorylated primers. Plasmids contained deletions of amino acids (aa) 2–17, 25–69, 75–144, 145–225, or 226–261. A plasmid containing F5L-GFP with a deletion of aa 315–322 was produced by splice overlap PCR using: CTCGCCCTTGCTCACTCTTTTGTACATCGATATCGC and **F5LRrev**, and **EGFPstop** and pGFP (external primers in bold), followed by cloning into pSSmCB linearized with *Eco*RI. 293A cells were infected with 50–100 p.f.u. of VACVWR or VACVWRΔF5L, then transfected 1 h later with 2 μg of plasmid DNA. Transfection media replaced after 3.5 h with phenol-red free D2-CMC. 48 h.p.i. fluorescent plaques were photographed.

Expression of F5 in uninfected cells

Full length (F5L) or truncated (F5L218) *F5L*, amplified from VACVWR DNA with: CGCGGGCCCGGGATCAACATTTATTAAACCGCATCAAG and either F5full: GGCGACCGGTGGATCGTTATCTATATGCCTGTACTTGGAT or F5218: GGCGACCGGTGGATCTGGAAACAGATAACAAGAAAACTCGTC, were cloned into pEGFP-N1. 293A cells were transfected with 2 μg of pEGFP-N1, pEGFP-N1::F5L, or pEGFP-N1::F5L218. Three hour post transfection, media was replaced with D2 for uninfected wells or VACVWRΔF5L or MVA (m.o.i=5). 1 h.p.i. inoculum was replaced with 2 ml/well phenol-red free D2. After overnight incubation at 37 °C, cells in the media were collected, while attached cells were washed with PBS and then removed using trypsin. Pooled cells were washed once with PBS, fixed using 1% PFA, and washed. eGFP fluorescence was measured using an LSR II flow cytometer (BD Biosciences) and data analyzed using FlowJo software (Tree Star Inc.). For inhibition

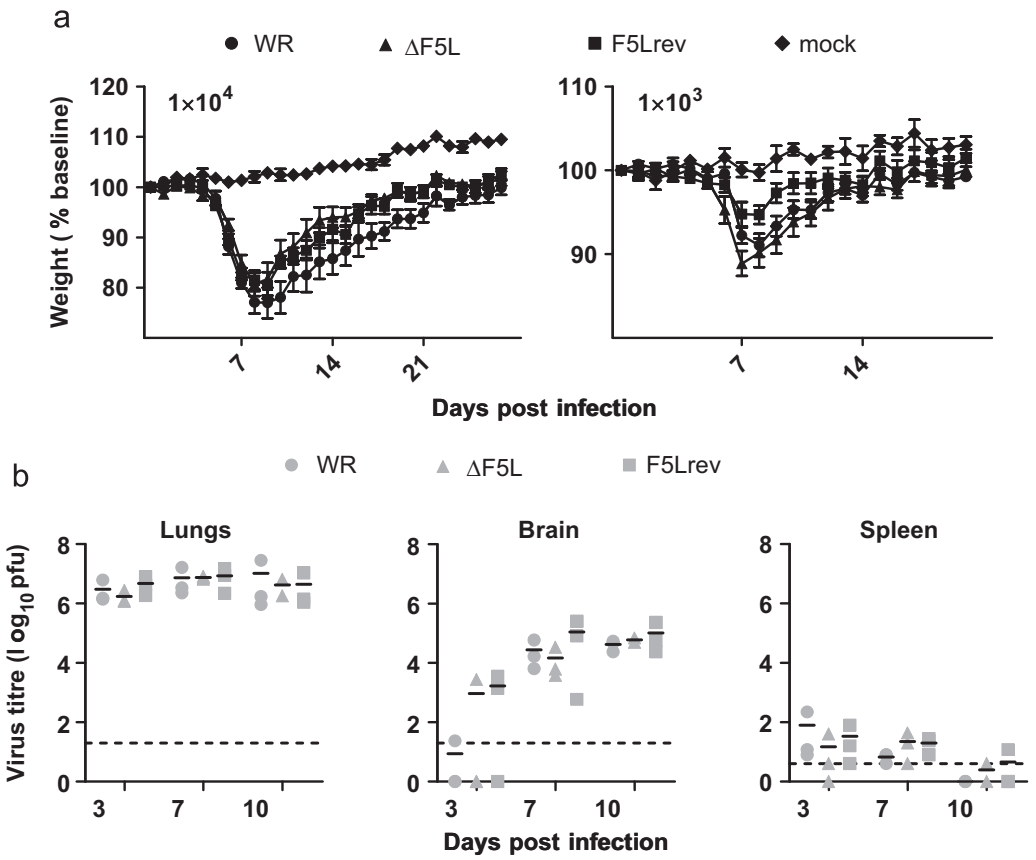

Fig. 8. Deletion of F5L does not affect the virulence of VACVWR after intranasal infection. (a) Groups of BALB/c mice received 1×10^4 (left) or 1×10^3 (right) p.f.u. of VACVWR, VACVWRΔF5L or VACVWRF5Lrev ($n=6$) or PBS (mock; $n=3$) intranasally and were weighed daily. Average weights ± SEM, expressed as a percentage of baseline are shown. In the 1×10^4 p.f.u. experiment, one mouse was euthanized from each infected group due to weight loss exceeding 30% of baseline (d9 for ΔF5L and F5Lrev and d10 for WR). Data are representative of 3 and 2 experiments with doses of 1×10^4 and 1×10^3 p.f.u., respectively. (b) Mice were infected with 1×10^4 p.f.u. and infectious titers determined on days 3, 7 and 10 p.i.. Titers for individual mice are shown by the symbols and averages with solid lines. The limit of detection (dashed line) was 20 p.f.u. for lungs and brain and 4 p.f.u. for spleen.

of intermediate and late gene expression, overnight media contained 40 μg ml^{-1} AraC.

Mice and infections

Mice were housed and all experiments carried out in compliance with ethical requirements under approval from the Animal Ethics and Experimentation Committee (ANU). Specific pathogen-free, female BALB/c mice were obtained from ARC (Perth, Australia) or APF (Canberra, Australia). For pathogenesis experiments, 8 week old mice were anesthetized by inhalation of isofluorane (4% in medical-grade oxygen at 0.8 l/min) and intradermally injected with 1×10^4 p.f.u. or 1×10^2 p.f.u. in 10 μl PBS in the left ear pinnae (Tscharke and Smith, 1999; Lin, Smith, and Tscharke, 2012), or infected intranasally with 1×10^4 p.f.u. or 1×10^3 p.f.u. in a total of 20 μl of PBS (10 μl per naris). For the dermal model, lesion sizes were estimated daily as described previously (Tscharke and Smith, 1999; Lin et al., 2012). After intranasal infection mice were weighed daily and monitored for signs of infection. Severely ill mice (clinical score >6) or those that lost more than 30% of baseline body weight that did not have an improving clinical score were euthanized.

Titration of virus from organs

The infected ears of intradermally infected mice were collected on day 5 p.i.. Organs were collected from intranasally infected mice at days 3, 7 or 10 p.i.. Ears or organs were homogenized in D2. Homogenates were frozen and thawed three times and sonicated for 20 s three times, before titration.

Statistical analysis

Statistical comparisons were done using Prism Software (version 5.01; GraphPad).

Acknowledgments

The authors thank Yik Chun Wong for assistance and advice with pathogenesis and immunology experiments; Bernard Moss for VACV strains WR, MVA, and the set of rescued MVA viruses; Michael Way for helpful comments on this manuscript; Giel van Dooren and Pritinder Kaur for primary HFF; Stewart Smith for general laboratory management; RSB animal services for husbandry of mice. Sequencing reactions were run by the ACRF Biomolecular Resource Facility, Canberra, Australia. This work was funded by the Australian NHMRC: #418108 and APP1023141 (DCT) and Australian ARC: FT110100310 (DCT) and DP1096623 (TPN).

Appendix A. Supporting information

Supplementary data associated with this article can be found in the online version at http://dx.doi.org/10.1016/j.virol.2014.03.020.

References

Alcamí, A., Smith, G.L., 1995. Vaccinia, cowpox, and camelpox viruses encode soluble gamma interferon receptors with novel broad species specificity. J. Virol. 69 (8), 4633–4639.

Almazan, F., Tscharke, D.C., Smith, G.L., 2001. The vaccinia virus superoxide dismutase-like protein (A45R) is a virion component that is nonessential for virus replication. J. Virol. 75 (15), 7018–7029.

Arakawa, Y., Cordeiro, J.V., Schleich, S., Newsome, T.P., Way, M., 2007a. The release of vaccinia virus from infected cells requires RhoA-mDia modulation of cortical actin. Cell Host Microbe 1 (3), 227–240.

Arakawa, Y., Cordeiro, J.V., Way, M., 2007b. F11L-mediated inhibition of RhoA-mDia signaling stimulates microtubule dynamics during Vaccinia virus infection. Cell Host Microbe 1 (3), 213–226.

Banham, A.H., Smith, G.L., 1993. Characterization of vaccinia virus gene B12R. J. Gen. Virol. 74 (Pt 12), 2807–2812.

Beard, P.M., Froggatt, G.C., Smith, G.L., 2006. Vaccinia virus kelch protein A55 is a 64 kDa intracellular factor that affects virus-induced cytopathic effect and the outcome of infection in a murine intradermal model. J. Gen. Virol. 87 (6), 1521–1529.

Bendtsen, J.D., Nielsen, H., von Heijne, G., Brunak, S., 2004. Improved prediction of signal peptides: SignalP 3.0. J. Mol. Biol. 340, 783–795.

Benfield, C.T.O., Ren, H., Lucas, S.J., Bahsoun, B., Smith, G.L., 2013. Vaccinia virus protein K7 is a virulence factor that alters the acute immune response to infection. J. Gen. Virol. 94 (Pt 7), 1647–1657.

Blanchard, T.J., Alcamí, A., Andrea, P., Smith, G.L., 1998. Modified vaccinia virus Ankara undergoes limited replication in human cells and lacks several immunomodulatory proteins: implications for use as a human vaccine. J. Gen. Virol. 79 (Pt 5), 1159–1167.

Blasco, R., Moss, B., 1991. Extracellular vaccinia virus formation and cell-to-cell virus transmission are prevented by deletion of the gene encoding the 37,000-Dalton outer envelope protein. J. Virol. 65 (11), 5910–5920.

Buller, R.M.L., Chakrabarti, S., Cooper, J.A., Twardzik, D.R., Moss, B., 1988. Deletion of the vaccinia virus growth factor gene reduces virus virulence. J. Virol. 62 (3), 866–874.

Carroll, M.W., Moss, B., 1997. Host range and cytopathogenicity of the highly attenuated MVA strain of vaccinia virus: propagation and generation of recombinant viruses in a nonhuman mammalian cell line. Virology 238 (2), 198–211.

Chen, R.A.-J., Jacobs, N., Smith, G.L., 2006. Vaccinia virus strain Western Reserve protein B14 is an intracellular virulence factor. J. Gen. Virol. 87 (6), 1451–1458.

Chen, R.A.J., Ryzhakov, G., Cooray, S., Randow, F., Smith, G.L., 2008. Inhibition of IκB kinase by vaccinia virus virulence factor B14. PLoS Pathog. 4 (2), e22.

Chung, C.S., Chen, C.H., Ho, M.Y., Huang, C.Y., Liao, C.L., Chang, W., 2006. Vaccinia virus proteome: identification of proteins in vaccinia virus intracellular mature virion particles. J. Virol. 80 (5), 2127–2140.

Cochran, M.A., Mackett, M., Moss, B., 1985. Eukaryotic transient expression system dependent on transcription factors and regulatory DNA sequences of vaccinia virus. Proc. Ntl. Acad. Sci. 82 (1), 19–23.

Cordeiro, J.V., Guerra, S., Arakawa, Y., Dodding, M.P., Esteban, M., Way, M., 2009. F11-Mediated Inhibition of RhoA Signalling Enhances the Spread of Vaccinia Virus *in vitro* and *in vivo* in an Intranasal Mouse Model of Infection. PLoS ONE 4 (12), e8506.

Dobson, B.M., Tscharke, D.C., 2014. Truncation of gene F5L partially masks rescue of vaccinia virus strain MVA growth on mammalian cells by restricting plaque size. J. Gen. Virol. 95 (2), 466–471.

Dodding, M.P., Newsome, T.P., Collinson, L.M., Edwards, C., Way, M., 2009. An E2-F12 complex is required for intracellular enveloped virus morphogenesis during vaccinia infection. Cell. Microbiol. 11 (5), 808–824.

Domi, A., Weisberg, A.S., Moss, B., 2008. Vaccinia virus E2L null mutants exhibit a major reduction in extracellular virion formation and virus spread. J. Virol. 82 (9), 4215–4226.

Drexler, I., Heller, K., Wahren, B., Erfle, V., Sutter, G., 1998. Highly attenuated modified vaccinia virus Ankara replicates in baby hamster kidney cells, a potential host for virus propagation, but not in various human transformed and primary cells. J. Gen. Virol. 79 (Pt 2), 347–352.

Duncan, S.A., Smith, G.L., 1992. Identification and characterization of an extracellular envelope glycoprotein affecting vaccinia virus egress. J. Virol. 66 (3), 1610–1621.

Engelstad, M., Smith, G.L., 1993. The Vaccinia Virus 42-kDa Envelope Protein Is Required for the Envelopment and Egress of Extracellular Virus and for Virus Virulence. Virology 194 (2), 627–637.

Fahy, A.S., Clark, R.H., Glyde, E.F., Smith, G.L., 2008. Vaccinia virus protein C16 acts intracellularly to modulate the host response and promote virulence. J. Gen. Virol. 89 (10), 2377–2387.

Finn, R.D., Mistry, J., Tate, J., Coggill, P., Heger, A., Pollington, J.E., Gavin, O.L., Gunesekaran, P., Ceric, G., Forslund, K., Holm, L., Sonnhammer, E.L., Eddy, S.R., Bateman, A., 2010. The Pfam protein families database. Nucleic Acids Res. 38, D211–D222.

Flesch, I.A., Wong, Y., Tscharke, D., 2012a. Analyzing CD8 T cells in mouse models of poxvirus infection. second ed. In: Isaacs, S.N. (Ed.), Vaccinia Virus and Poxvirology: Methods and Protocols, Vol. 890. Humana Press, pp. 199–218.

Flesch, I.E.A., Hollett, N.A., Wong, Y.C., Tscharke, D.C., 2012b. Linear fidelity in quantification of anti-viral $CD8^+$ T cells. PLoS ONE 7 (6), e39533.

Handa, Y., Durkin, Charlotte, H., Dodding, Mark P., Way, M., 2013. Vaccinia virus F11 promotes viral spread by acting as a PDZ-containing scaffolding protein to bind myosin-9A and inhibit RhoA signaling. Cell Host Microbe 14 (1), 51–62.

Krogh, A., Larsson, B.r., von Heijne, G., Sonnhammer, E.L.L., 2001. Predicting transmembrane protein topology with a hidden markov model: application to complete genomes. J. Mol. Biol. 305 (3), 567–580.

Lin, L.C.W., Smith, S.A., Tscharke, D.C., 2012. An intradermal model for vaccinia virus pathogenesis in mice. second ed. In: Isaacs, S.N. (Ed.), Vaccinia Virus and Poxvirology: Methods and Protocols, Vol. 890. Humana Press, Totowa, N.J., pp. 147–159.

Manes, N.P., Estep, R.D., Mottaz, H.M., Moore, R.J., Clauss, T.R., Monroe, M.E., Du, X., Adkins, J.N., Wong, S.W., Smith, R.D., 2008. Comparative proteomics of human monkeypox and vaccinia intracellular mature and extracellular enveloped virions. J. Proteome Res. 7 (3), 960–968.

McCraith, S., Holtzman, T., Moss, B., Fields, S., 2000. Genome-wide analysis of vaccinia virus protein-protein interactions. Proc. Natl. Acad. Sci. U. S. A. 97 (9), 4879–4884.

McIntosh, A., Smith, G., 1996. Vaccinia virus glycoprotein A34R is required for infectivity of extracellular enveloped virus. J. Virol. 70 (1), 272–281.

Melamed, S., Wyatt, L.S., Kastenmayer, R.J., Moss, B., 2013. Attenuation and immunogenicity of host-range extended modified vaccinia virus Ankara recombinants. Vaccine 31 (41), 4569–4577.

Morales, I., Carbajal, M.A., Bohn, S., Holzer, D., Kato, S.E.M., Greco, F.A.B., Moussatche, N., Locker, J.K., 2008. The vaccinia virus F11L gene product facilitates cell detachment and promotes migration. Traffic 9 (8), 1283–1298.

Morgan, G.W., Hollinshead, M., Ferguson, B.J., Murphy, B.J., Carpentier, D.C., Smith, G.L., 2010. Vaccinia protein F12 has structural similarity to Kinesin light chain and contains a motor binding motif required for virion export. PLoS Pathog. 6 (2), e1000785.

Olson, V.A., Karem, K.L., Smith, S.K., Hughes, C.M., Damon, I.K., 2009. Smallpox virus plaque phenotypes: genetic, geographical and case fatality relationships. J. Gen. Virol. 90 (Pt 4), 792–798.

Parkinson, J.E., Sanderson, C.M., Smith, G.L., 1995. The vaccinia virus A38l gene-product is a 33-Kda integral membrane glycoprotein. Virology 214 (1), 177–188.

Parkinson, J.E., Smith, G.L., 1994. Vaccinia virus gene A36R encodes a Mr 43-50 K protein on the surface of extracellular enveloped virus. Virology 204 (1), 376–390.

Pires de Miranda, M., Reading, P.C., Tscharke, D.C., Murphy, B.J., Smith, G.L., 2003. The vaccinia virus kelch-like protein C2L affects calcium-independent adhesion to the extracellular matrix and inflammation in a murine intradermal model. J. Gen. Virol. 84, 2459–2471.

Price, N., Tscharke, D.C., Smith, G.L., 2002. The vaccinia virus B9R protein is a 6 kDa intracellular protein that is non-essential for virus replication and virulence. J. Gen. Virol. 83 (4), 873–878.

Rasband, W.S., 1997-2012. Image J. U.S. National Institutes of Health. Bethesda, Maryland, USA ⟨http://imagej.nih.gov/ij/⟩.

Reading, P.C., Smith, G.L., 2003. A kinetic analysis of immune mediators in the lungs of mice infected with vaccinia virus and comparison with intradermal infection. J. Gen. Virol. 84 (Pt 8), 1973–1983.

Resch, W., Hixson, K.K., Moore, R.J., Lipton, M.S., Moss, B., 2007. Protein composition of the vaccinia virus mature virion. Virology 358 (1), 233–247.

Roberts, K.L., Smith, G.L., 2008. Vaccinia virus morphogenesis and dissemination. Trends Microbiol. 16 (10), 472–479.

Rodriguez, J.F., Smith, G.L., 1990. IPTG-dependent vaccinia virus: identification of a virus protein enabling virion envelopment by Golgi membrane and egress. Nucleic Acids Res. 18 (18), 5347–5351.

Roper, R.L., Wolffe, E.J., Weisberg, A., Moss, B., 1998. The envelope protein encoded by the A33R gene is required for formation of actin-containing microvilli and efficient cell-to-cell spread of vaccinia virus. J. Virol. 72 (5), 4192–4204.

Roseman, N.A., Slabaugh, M.B., 1990. The vaccinia virus HindIII F fragment: nucleotide sequence of the left 6.2 kb. Virology 178 (2), 410–418.

Sakala, I.G., Chaudhri, G., Buller, R.M., Nuara, A.A., Bai, H., Chen, N., Karupiah, G., 2007. Poxvirus-encoded gamma interferon binding protein dampens the host immune response to infection. J. Virol. 81 (7), 3346–3353.

Sanderson, C.M., Smith, G.L., 1998. Vaccinia virus induces $Ca2+-$independent cell-matrix adhesion during the motile phase of infection. J. Virol. 72 (12), 9924–9933.

Schmelz, M., Sodeik, B., Ericsson, M., Wolffe, E.J., Shida, H., Hiller, G., Griffiths, G., 1994. Assembly of vaccinia virus: the second wrapping cisterna is derived from the trans Golgi network. J. Virol. 68 (1), 130–147.

Schweneker, M., Lukassen, S., Spath, M., Wolferstatter, M., Babel, E., Brinkmann, K., Wielert, U., Chaplin, P., Suter, M., Hausmann, J., 2012. The vaccinia virus O1 protein is required for sustained activation of extracellular signal-regulated kinase 1/2 and promotes viral virulence. J. Virol. 86 (4), 2323–2336.

Staib, C., Drexler, I., Sutter, G., 2004. Construction and isolation of recombinant MVA. In: Isaacs, S.N. (Ed.), Vaccinia Virus and Poxvirology: Methods and Protocols, Vol. 269. Humana Press, Clifton, NJ, pp. 77–99.

Symons, J.A., Tscharke, D.C., Price, N., Smith, G.L., 2002. A study of the vaccinia virus interferon-γ receptor and its contribution to virus virulence. J. Gen. Virol. 83 (Pt 8), 1953–1964.

Tscharke, D.C., Reading, P.C., Smith, G.L., 2002. Dermal infection with vaccinia virus reveals roles for virus proteins not seen using other inoculation routes. J. Gen. Virol. 83, 1977–1986.

Tscharke, D.C., Smith, G.L., 1999. A model for vaccinia virus pathogenesis and immunity based on intradermal injection of mouse ear pinnae. J. Gen. Virol. 80, 2751–2755.

Upton, C., Slack, S., Hunter, A.L., Ehlers, A., Roper, R.L., 2003. Poxvirus orthologous clusters: toward defining the minimum essential poxvirus genome. J. Virol. 77 (13), 7590–7600.

Valderrama, F., Cordeiro, J.V., Schleich, S., Frischknecht, F., Way, M., 2006. Vaccinia virus-induced cell motility requires F11L-mediated inhibition of RhoA signaling. Science 311 (5759), 377–381.
van Eijl, H., Hollinshead, M., Rodger, G., Zhang, W.H., Smith, G.L., 2002. The vaccinia virus F12L protein is associated with intracellular enveloped virus particles and is required for their egress to the cell surface. J. Gen. Virol. 83 (Pt 1), 195–207.
Ward, B.M., Moss, B., 2001. Vaccinia virus intracellular movement is associated with microtubules and independent of actin tails. J. Virol. 75 (23), 11651–11663.
Welch, Matthew D., Way, M., 2013. Arp2/3-mediated actin-based motility: a tail of pathogen abuse. Cell Host Microbe 14 (3), 242–255.
Wolffe, E., Katz, E., Weisberg, A., Moss, B., 1997. The A34R glycoprotein gene is required for induction of specialized actin-containing microvilli and efficient cell-to-cell transmission of vaccinia virus. J. Virol. 71 (5), 3904–3915.
Wolffe, E.J., Isaacs, S.N., Moss, B., 1993. Deletion of the vaccinia virus B5R gene encoding a 42-kilodalton membrane glycoprotein inhibits extracellular virus envelope formation and dissemination. J. Virol. 67 (8), 4732–4741.
Wolffe, E.J., Weisberg, A.S., Moss, B., 1998. Role for the vaccinia virus A36R outer envelope protein in the formation of virus-tipped actin-containing microvilli and cell-to-cell virus spread. Virology 244 (1), 20–26.
Wong, Y.C., Lin, L.C.W., Melo-Silva, C.R., Smith, S.A., Tscharke, D.C., 2011. Engineering recombinant poxviruses using a compact GFPâ€“blasticidin resistance fusion gene for selection. J. Virol. Methods 171 (1), 295–298.
Wyatt, L.S., Carroll, M.W., Czerny, C.P., Merchlinsky, M., Sisler, J.R., Moss, B., 1998. Marker rescue of the host range restriction defects of modified vaccinia virus Ankara. Virology 251 (2), 334–342.
Yang, Z., Bruno, D.P., Martens, C.A., Porcella, S.F., Moss, B., 2010. Simultaneous high-resolution analysis of vaccinia virus and host cell transcriptomes by deep RNA sequencing. Proc. Natl. Acad. Sci. U. S. A. 107 (25), 11513–11518.
Yoder, J.D., Chen, T.S., Gagnier, C.R., Vemulapalli, S., Maier, C.S., Hruby, D.E., 2006. Pox proteomics: mass spectrometry analysis and identification of Vaccinia virion proteins. Virol. J. 3, 10.
Zhang, W.H., Wilcock, D., Smith, G.L., 2000. Vaccinia virus F12L protein is required for actin tail formation, normal plaque size, and virulence. J. Virol. 74 (24), 11654–11662.
Zwilling, J., Sliva, K., Schwantes, A., Schnierle, B., Sutter, G., 2010. Functional F11L and K1L genes in modified vaccinia virus Ankara restore virus-induced cell motility but not growth in human and murine cells. Virology 404 (2), 231–239.